Journal of Medicinal Chemistry

Drug Annotation

pubs.acs.org/jmc

Discovery of a 9-mer Cationic Peptide (LTX-315) as a Potential First in Class Oncolytic Peptide

Bengt Erik Haug,*[,†,‡,⊥] Ketil André Camilio,[†,§] Liv Tone Eliassen,[†,#] Wenche Stensen,[†,¶] John Sigurd Svendsen,[†,¶] Kristel Berg,[†,∇] Bjarte Mortensen,[†] Guillaume Serin,[∥] Jean-Francois Mirjolet,[∥] Francis Bichat,[∥] and Øystein Rekdal*[,†,§]

[†]Lytix Biopharma AS, Sykehusveien 21, NO-9294 Tromsø, Norway

[‡]Department of Chemistry and Centre for Pharmacy, University of Bergen, Allégaten 41, NO-5007 Bergen, Norway

[§]Department of Medical Biology, Faculty of Health Sciences, UiT The Arctic University of Norway, NO-9037 Tromsø, Norway

[∥]Oncodesign, 21076 Dijon, France

[¶]Department of Chemistry, UiT The Arctic University of Norway, NO-9037 Tromsø, Norway

Supporting Information

ABSTRACT: Oncolytic immunotherapies represent a new promising strategy in the treatment of cancer. In our efforts to develop oncolytic peptides, we identified a series of chemically modified 9-mer cationic peptides that were highly effective against both drug-resistant and drug-sensitive cancer cells and with lower toxicity toward normal cells. Among these peptides, LTX-315 displayed superior anticancer activity and was selected as a lead candidate. This peptide showed relative high plasma protein binding abilities and a human plasma half-life of 160 min, resulting in formation of nontoxic metabolites. In addition, the lead candidate demonstrated relatively low ability to inhibit CYP450 enzymes. Collectively these data indicated that this peptide has potential to be developed as a new anticancer agent for intratumoral administration and is currently being evaluated in a phase I/IIa study.

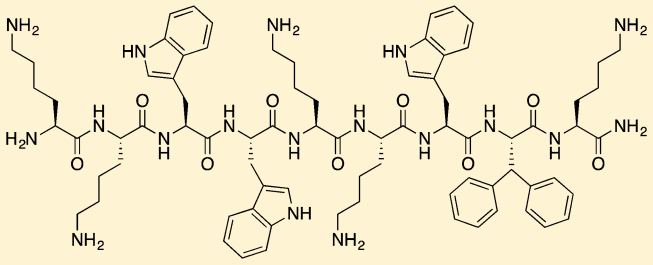

INTRODUCTION

Modern cancer therapy has experienced a shift from systemic treatment using cytotoxic chemotherapeutics to therapies targeting the immune system.[1] Cancer immunotherapies either stimulate specific components of the immune system or counteract signals produced by cancer cells that suppress immune responses. Combinations of these complementary immunotherapy treatments are expected to be an integral part of future cancer treatment delivering significant clinical benefit.

An alternative approach to stimulate the immune system is the use of oncolytic immunotherapies. Oncolytic viruses have emerged as a new and promising strategy with significant clinical responses in cancer patients,[2] and very recently the oncolytic virus Imlygic (talimogene laherparepvec)[3] was approved by the U.S. Food and Drug Administration for the treatment of patients with unresectable melanoma. Oncolytic peptides offer yet a new therapeutic modality,[4] and their membranolytic mode of action includes the release of danger-associated molecular pattern molecules (DAMPs)[5] and tumor antigens from cancer cells, resulting in regression of solid tumors and systemic tumor specific immune responses.[6,7] Consequently, the development of oncolytic peptides into novel anticancer therapeutics has emerged as a promising immunotherapeutic strategy.[8] Toward this end, peptide **5** (LTX-315,[7] Table 1) has undergone a phase I study designed to evaluate safety profile and determine a recommended dose, where main safety issues below MTD were mostly local adverse events and flushing.[9] Peptide **5** is currently tested in clinical phase I/IIa studies, as a potential first-in-class oncolytic peptide.[10]

Peptide **5** is the culmination of our efforts over a number of years into the design of novel and more optimized antimicrobial and anticancer peptides, coined by our interest in the host defense peptide (HDP) bovine lactoferricin (LFcinB).[11−13] HDPs have been found in a wide variety of species as part of the organisms' defense system against pathogens,[14,15] and it is not uncommon for these cationic peptides, including LFcinB and derivatives,[16−20] to also demonstrate cytotoxic activity against cancer cells at concentrations that are not toxic to normal cells.[21−23] Their biological activity is often ascribed to peptide−membrane interactions in addition to possible intracellular targets.[24−32] Negatively charged constituents on bacterial cell surfaces and a higher abundance of anionic constituents on the outer leaflet of cancer cell membranes compared to normal cell membranes[33] have been implied to explain the peptide−membrane interactions.

Received: December 30, 2015

 © XXXX American Chemical Society

DOI: 10.1021/acs.jmedchem.5b02025
J. Med. Chem. XXXX, XXX, XXX−XXX

Table 1. Sequences of 9-mers and Initial Screening Data

compd	sequence[a]	IC_{50} ± SD (μM)[b]		
		MRC-5	A20	AT84
1	Lys-Lys-Trp-Trp-Lys-Lys-Trp-Trp-Lys-NH_2	>357[c]	37.3 ± 1.5	31.0 ± 1.0
2	Lys-Lys-Dip-Trp-Lys-Lys-Trp-Trp-Lys-NH_2	488 ± 52	51.7 ± 6.5	36.7 ± 9.5
3	Lys-Lys-Trp-Dip-Lys-Lys-Trp-Trp-Lys-NH_2	287 ± 52	25.7 ± 0.6	24.7 ± 2.3
4	Lys-Lys-Trp-Trp-Lys-Lys-Dip-Trp-Lys-NH_2	102 ± 7.6	12.3 ± 1.5	25.3 ± 4.2
5[7]	Lys-Lys-Trp-Trp-Lys-Lys-Trp-Dip-Lys-NH_2	34.3 ± 2.3	8.3 ± 1.2	11.0 ± 0
6	Lys-Lys-Trp-Dip-Lys-Lys-Trp-Dip-Lys-NH_2	80.0 ± 7.0	12.0 ± 0	15.0 ± 1.0
7	Lys-Lys-Trp-Bip-Lys-Lys-Trp-Trp-Lys-NH_2	174 ± 22	18.7 ± 1.5	27.3 ± 5.1
8	Lys-Lys-Trp-1-Nal-Lys-Lys-Trp-Trp-Lys-NH_2	238 ± 69	24.0 ± 1.0	26.3 ± 7.1
9	Lys-Lys-Trp-2-Nal-Lys-Lys-Trp-Trp-Lys-NH_2	257 ± 20	26.0 ± 1.7	29.3 ± 7.8
10	Lys-Lys-Trp-9-Ath-Lys-Lys-Trp-Trp-Lys-NH_2	40.0 ± 1.7	9.3 ± 1.2	11.0 ± 1.0
11	Lys-Lys-Bip-Trp-Lys-Lys-Trp-Trp-Lys-NH_2	151 ± 16	13.0 ± 1.0	17.7 ± 3.1
12	Lys-Lys-Bip-Trp-Lys-Lys-Trp-Trp-Lys-NH_2	87.0 ± 15.1	8.3 ± 1.5	11.3 ± 1.2
13	Orn-Orn-Trp-Dip-Orn-Orn-Trp-Trp-Orn-NH_2	323 ± 33	21.7 ± 2.5	23.0 ± 3.6
14	Dab-Dab-Trp-Dip-Dab-Dab-Trp-Trp-Dab-NH_2	97.7 ± 5.1	8.3 ± 0.6	14.3 ± 1.2
15	Dap-Dap-Trp-Dip-Dap-Dap-Trp-Trp-Dap-NH_2	516 ± 5.2	67.7 ± 13.2	154 ± 29
16	Arg-Arg-Trp-Dip-Arg-Arg-Trp-Trp-Arg-NH_2	76.0 ± 9.5	6.7 ± 1.2	11.3 ± 2.1
17	lys-lys-Trp-Dip-lys-lys-Trp-Trp-lys-NH_2	>347[c]	134 ± 13	113 ± 10
18[6]	Trp-Lys-Lys-Trp-Dip-Lys-Lys-Trp-Lys-NH_2	122 ± 16	16.0 ± 3.0	21.0 ± 1.7

[a]Amino acids with small first letters are of (*R*)-configuration. Structures of unnatural amino acids are shown in Figure 2. [b]Inhibitory concentration killing 50% of the cells (IC_{50}). Data from three or more independent measurements are presented as mean ± SD. [c]IC_{50} above maximum concentration tested.

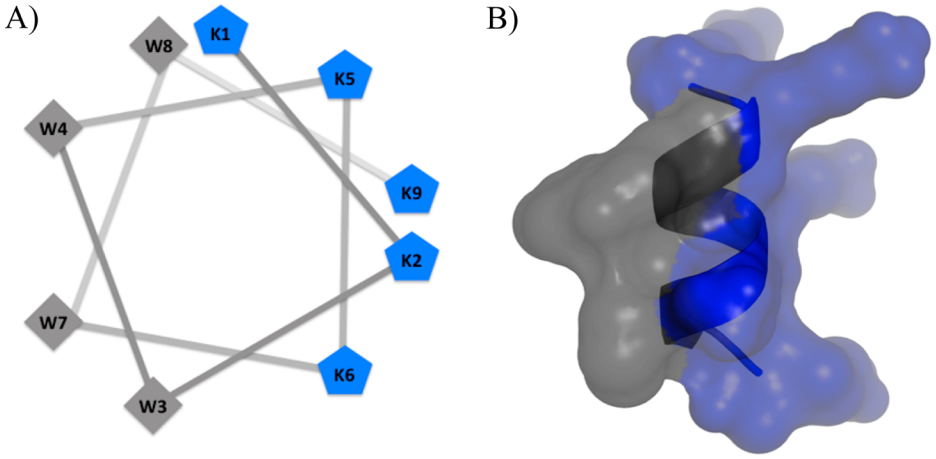

Figure 1. Structural representations of (A) an idealized helical wheel projection of peptide **1** with Lys residues in blue and Trp residues in gray (generated using Helical Wheel Projections, version Id: wheel.pl,v 1.4) and (B) secondary structure model of peptide **5** (generated using PyMOL 1.3) illustrating the surface charge of an idealized amphipathic conformation with Lys residues (in blue) on one side and aromatic residues (in gray) on the opposite side.

In addition to inherently being rich in basic amino acids (Lys and Arg), cationic antimicrobial and anticancer peptides have a high content of hydrophobic residues (Trp, Phe, Leu, and Ile). Upon interaction with negatively charged membranes the formation of amphipathic structures with separated cationic and hydrophobic regions has been described.[34−37] It has also recently been shown that short amphipathic antimicrobial peptides can be constructed using noncoded lipophilic amino acids,[38] and use of $\beta^{2,2}$-amino acids has yielded antimicrobial and anticancer peptides and peptidomimetics.[39−42]

We have found that the nature, size, and positioning of aromatic amino acids are critical for activity and that a high net positive charge and the size of the cationic sector also strongly influence the activity.[35,43−45] This has enabled the de novo design of 9-mer cationic peptides where counterproductive structural elements have been deleted, enabling further optimization of features identified as important for anticancer activity. An array of cationic 9-mer peptides that consist of five cationic residues, two or three tryptophan residues, and one or two bulky and lipophilic unnatural amino acids (see Figures 1 and 2) were evaluated for their cytotoxic activity. Five peptides were chosen as a lead series and were tested against a wider range of cancer cell lines, including drug-resistant cell lines. On the basis of these data, peptide **5** was chosen as a lead candidate for preclinical and clinical studies.

■ RESULTS AND DISCUSSION

The design of peptide **5** was a result of our systematic SAR studies on cationic anticancer peptides. Through these studies, we landed on cationic 9-mer peptides based on $(KKWW)_2K$-NH_2 (peptide **1**), which has a net positive charge of +6 at physiological pH. Peptide **1** is modeled as an α-helical

DOI: 10.1021/acs.jmedchem.5b02025
J. Med. Chem. XXXX, XXX, XXX−XXX

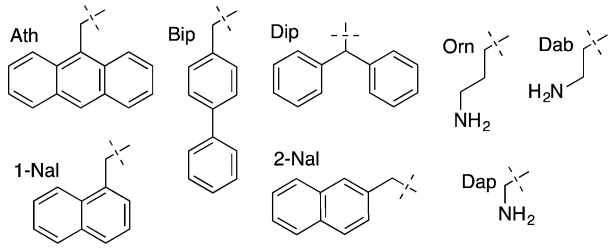

Figure 2. Structure of amino acid side chains.

amphipathic structure with its cationic residues positioned on one side of the helix and the aromatic residues sequestered to the other side (Figure 1).[7] Peptides with this class of sequence in a helical conformation will enable efficient interaction with anionic membranes.

Design of Peptides for a Lead Series: Role of Aromatic Amino Acids. Peptide **1** (Table 1), with only Trp as the hydrophobic amino acid, was found to be active against the human A20 lymphoma and the murine AT84 squamous cell carcinoma cancer cell lines and showed no toxicity toward normal human fibroblasts (MRC-5 cells, Table 1). We have previously shown that replacement of the Trp residues of 15-mer lactoferricin peptides with larger noncoded hydrophobic amino acids leads to an increased cytotoxic activity,[43] and we therefore proceeded to insert a 3,3-diphenylalanine (Dip) residue (see Figure 2) at either of the aromatic positions of peptide **1**, giving peptides **2**−**5**. Interestingly, the replacement of Trp8 with Dip to give peptide **5** resulted in high activity against both A20 and AT84 cancer cell lines but at the expense of increased toxicity against MRC-5 cells. Introduction of Dip in position 7 (peptide **4**) also gave a significant increase in activity toward both the cancerous A20 and the noncancerous MRC-5 cell lines. Noteworthy, the Trp3 to Dip3 (peptide **2**) replacement resulted in a slight loss of activity against the cancer cell lines, while the introduction of Dip in position 4 (peptide **3**) gave a slight increased activity. Introduction of two Dip residues (position 4 and 8) as in peptide **6** did not further increase the anticancer activity.

We have previously shown that the position of Trp residues significantly influenced the anticancer activity of idealized helical model peptides based on the $(KAAKKAA)_3$ sequence. Their structure in the presence of artificial anionic cell membranes was also found to be highly dependent on the position of Trp.[35] For these 21-mer peptides, replacement of Ala residues with Trp residues at either flank of the cationic sector gave increased cytotoxic activity compared to replacing Ala residues opposite to the cationic sector. For a number of antimicrobial and anticancer peptides, we have seen that replacement of a Trp residue with the bulky Dip residue has a positive impact on activity and we were therefore surprised to see that a Dip residue in position 3 appeared counterproductive for the 9-mers. Clearly, the position of the noncoded bulky aromatic residue significantly influenced the activity of the resulting peptides and the Trp to Dip modification was more beneficial at the C-terminal of the 9-mers.

Next, we opted to investigate the use of different unnatural aromatic amino acids. Peptide **3** was chosen as the model peptide, since we did see an improvement in activity resulting from the Trp4 to Dip4 replacement but not as pronounced as for positions 7 and 8. Introduction of biphenylalanine (Bip), 1-naphthylalanine (1-Nal), or 2-naphthylalanine (2-Nal) gave peptides **7**−**9**, respectively (see Figure 2 for structures), which showed more or less the same activity as peptide **3**. However, peptide **10**, with a 9-anthracenylalanine (Ath) residue in position 4, was found to be significantly more active. Interestingly, while the Ath and Dip side chains have quite similar structural properties,[46] particularly the width of the side chains (7.3 and 7.1 Å, respectively), their contribution to the cytotoxic activity of the peptides differed. The effect of changing from Dip to Bip was found to be dependent on the position; i.e., changing Dip4 to Bip (peptides **3** and **7**) only moderately changed the activity against the A20 cell line, whereas the same change in position 3 (peptides **2** and **11**) resulted in a substantial change in overall cytotoxic activity. Clearly the broad Dip side chain is a poor fit for the 3 position, while introduction of the narrow and long Bip side chain[46] results in increased activity compared to the parent peptide. It is quite possible that the overall structure of the peptides in their active conformation will differ and that the nature of the unnatural amino acid and also the position of the particular amino acid may have an influence in this respect.

Design of Peptides for Lead Series: Role of Cationic Amino Acids. We also investigated the use of different cationic amino acids for the 9-mers (see Table 1 and Figure 2), and peptide **3** was again chosen as the model peptide. As manipulation with a single cationic residue was expected to have a low effect on biological activity, all Lys residues were replaced in each analog. The carbon side chain of the cationic amino acids in the peptides was shortened sequentially by one carbon atom going from peptide **3** through peptides **13** and **14**. Interestingly, a shorter side chain of the cationic amino acid had a positive effect on the cytotoxic activity and particularly the introduction of the 2,4-diaminobutanoic acid (Dab) residue inferred high cytotoxic activity. Shortening the side chain length further by including 2,3-diaminopropionic acid (Dap) residues however had a detrimental effect on the activity, possibly due to the lower basicity of Dap compared to the Lys, Orn, and Dab residues,[47,48] which may prevent the Dap side chains of peptide **15** from being charged under the assay conditions. For the peptides investigated in this study, it is clear that a short distance between the peptide backbone and the positively charged amine group of Dab was beneficial for activity.

Arg residues have earlier been reported to confer higher toxicity when replacing Lys residues in an antimicrobial peptide,[49] and in our case peptide **16** which contains Arg residues instead of Lys residues was found to be more active albeit also more toxic to MRC-5 cells than the Lys-containing peptide **3**. This effect has been attributed to the multidimensional charge and ability to interact with multiple phospholipid head groups of the Arg guanidine moiety.[49−51] Interestingly, the Dab-containing **14** and Arg-containing **16** peptides displayed similar activity against the three cell lines (Table 1).

The structure of the active conformation of the peptides may change depending on the nature of the cationic amino acids introduced, and the low activity of peptide **17** (five D-Lys residues) illustrates that the structure is an important feature of the peptides. While the $(KKWW)_2K$ sequence may adopt a perfect amphipathic helical structure, it is not known whether this is the preferred conformation in a peptide−lipid complex and further studies into this will be reported in due course.

Peptide Lead Series: Cancer Cell Panel Screening. On the basis of the results from the peptides presented and discussed above, we decided to expand our panel of cancer cells and selected five peptides as a lead series for further investigations. The five candidates were chosen based on the

DOI: 10.1021/acs.jmedchem.5b02025
J. Med. Chem. XXXX, XXX, XXX−XXX

Table 2. Results from Panel Screening of Human Cancer and Normal Cell Lines IC_{50} in (μM)[a]

Origin (number)	5	11	12	16	18
Blood (7)	2-3	4-8	4-8	4-8	5-10
Brain (3)	3-7	6-18	6-17	5-13	10-17
Breast (5)	1-4	4-11	2-10	4-8	5-14
Colon (4)	3-4	5-14	6-10	5-12	9-12
Kidney (2)	3-6	8-17	6-14	6-8	14-19
Liver (2)	5-7	13-15	8-9	6-17	16-20
Lung (3)	2-3	6-11	5-9	6-9	7-10
Lymphoma (10)	1-5	4-16	3-9	2-11	5-13
Ovary (4)	3-7	7-18	7-14	5-11	6-20
Pancreas (2)	4	9-11	8-10	6-12	17-18
Prostate (2)	4	9	8-10	7-10	12-14
Skin (3)	3-5	7-13	7-11	6-11	12-18
Normal (2)	9-16	31-38	28-33	15-19	28-56

[a]Cytotoxic activity given as the range in mean inhibitory concentration killing 50% of the cells (IC_{50}) measured for cell lines of the same histological origin. Color-coding: Green = mean IC_{50} < 5, yellow = mean IC_{50} = 5−15, red = mean IC_{50} > 15. See Supporting Information Table S3 for the full data set.

Table 3. Activity against Drug Sensitive and Drug Resistant Tumor Cell Lines (IC_{50} ± SD in μM)[a]

cell line	5	11	12	16	18
HL-60	2.1 ± 0.4	6.1 ± 1.8	6.1 ± 3.4	6.7 ± 3.7	8.0 ± 1.1
HL-60/ADR[b]	3.0 ± 0.9	7.0 ± 3.7	4.9 ± 3.7	6.0 ± 4.5	10.5 ± 3.1
MCF-7	2.2 ± 0.6	6.8 ± 2.8	4.6 ± 1.1	5.5 ± 0.9	8.9 ± 2.8
MCF-7/mdr[c]	2.5 ± 1.0	8.4 ± 2.7	4.9 ± 1.6	6.6 ± 2.8	11.0 ± 4.4
IGROV-1	6.4 ± 2.0	13.4 ± 1.6	14.3 ± 5.3	11.1 ± 3.4	19.6 ± 8.7
IGROV-1/CDDP[d]	3.2 ± 1.6	6.6 ± 2.6	6.6 ± 2.7	5.5 ± 2.2	6.4 ± 2.6
K-562	3.0 ± 0.3	7.2 ± 0.4	7.4 ± 0.1	7.0 ± 0.8	8.2 ± 1.3
K562/Gleevec[e]	3.0 ± 0.3	7.9 ± 2.9	7.6 ± 1.3	7.7 ± 1.6	9.0 ± 2.1

[a]Inhibitory concentration killing 50% of the cells (IC_{50}). Data from three independent measurements are presented as the mean ± SD. [b]The HL-60/ADR cell line is resistant to the cancer drug adriamycin. [c]The MCF-7/mdr cell line is transfected with a gene denoted Multi-Drug Resistance 1 which infers resistance toward several cancer drugs. [d]The IGROV-1/CDDP ovarian cancer cell line is resistant to cisplatin. [e]The K562/Gleevec cell line is resistant to the cancer drug imatinib.

overall anticancer activity, sequence, nature of the unnatural aromatic amino acid, nature of the cationic amino acid, and stability toward proteolytic degradation (D-peptide). Since peptide **18** (LTX-302,[6] see Table 1) had shown anticancer activity in a murine lymphoma model,[6] it was included in the screening. In addition, the highly active peptide **5** and peptide **11**, which contain different unnatural amino acids (Dip and Bip, respectively), were included. Even though peptide **14**, containing Dab residues instead of Lys, also displayed high cytotoxic activity and slightly lower toxicity, it was not considered for the lead series as it contains six noncoded amino acids. This decision was based on cost of goods considerations (protected Dab is at least 10 times more expensive than protected Lys) and the potential release of noncoded amino acids upon hydrolysis of the peptide chain. We also included peptide **12**, which is the enantiomer of **11** in order to elucidate whether the slightly higher activity for the D-peptide and the invoked higher enzymatic stability would be beneficial. Finally, we included peptide **16**, which was the only Arg-containing peptide of this study.

The lead series was submitted to a panel screening of 10 human lymphoma cell lines, 37 human cancer cell lines from different origins, and 2 normal cell lines (see Table S2 in Supporting Information for description of cell lines). A summary of the mean IC_{50} range for each peptide in the lead series toward cell lines of different histological origin is presented in Table 2 (see Table S3 for the complete data set). The expanded screening shows that all peptides in the lead series were highly active against a vast range of cancer cells. It is interesting to note that the two enantiomeric peptides **11** and **12** displayed essentially the same range of activity. Peptide **12**, however, is expected to have a higher overall activity in tumor models in vivo. Peptide **5** was clearly the most active peptide in the panel screening, with mean IC_{50} values 2- to 4-fold lower than for the other four peptides, while peptide **18** was overall least active. Even though peptide **5** displayed highest activity against the two normal cell lines (HUV-EC-C and MRC-5), the tumor cell/normal cell specificity ratio was not lower than for the other peptides in the lead series.

Peptide Lead Series: Activity toward Drug-Resistant Cancer Cells. Drug resistance is one of the main causes of failure in cancer chemotherapy. Hence, several drug-sensitive and drug-resistant cancer cell pairs were included in the panel screening. The drug-resistant cell lines that were included

DOI: 10.1021/acs.jmedchem.5b02025
J. Med. Chem. XXXX, XXX, XXX−XXX

represent different types of common resistance mechanisms for cancer cells (see Table 3 for details). Intriguingly, each of the five peptides displayed almost similar activity against the drug-resistant and drug-sensitive cell lines, including multidrug-resistant phenotypes (see Table 3 and Table S2). Hence, peptide **5** may have the potential to be used in treating tumors that are or have become resistant to conventional chemotherapy.

The screening of the lead series against sensitive and drug-resistant cancer cell lines clearly shows that peptide **5** is overall the most active peptide, and it was therefore selected for further preclinical studies.

Preclinical Studies: Plasma Stability, Protein Binding, and Partitioning. Peptide **5** has been designed for intratumoral administration; however injection of a relative high local concentration of peptide **5** could cause leakage into systemic circulation. We therefore investigated in vitro stability in human plasma as well as plasma protein binding properties and plasma/blood cell partitioning of peptide **5** in rats, dogs, and humans.

The stability of peptide **5** when exposed to human plasma was monitored using HPLC (Figure 3), which revealed that

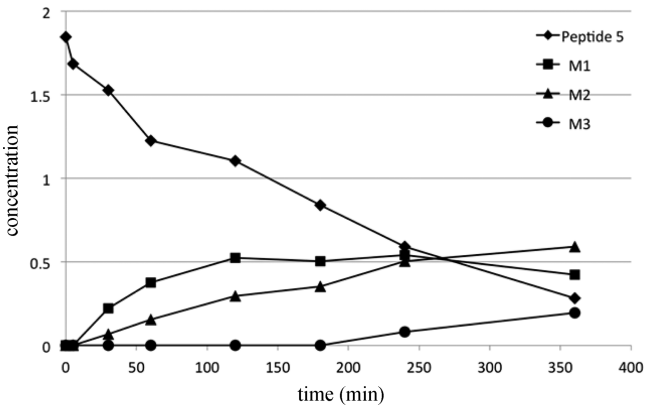

Figure 3. Metabolism of peptide **5**.

three different metabolites were formed (**M1**−**M3**, Table 5) as a result of sequential exopeptidase-mediated cleavage from the N-terminal. The half-life of peptide **5** was determined to be 160 min. In order to test whether the three metabolites would contribute to the anticancer effect of a given dose of peptide **5**, the metabolites were synthesized and tested for cytotoxic activity against MRC-5 and A20 cells (Table 5). Interestingly, the sequential breakdown of peptide **5** leads to a gradual loss of activity against the cancer cell line, with a simultaneous reduction in toxicity toward fibroblasts. On the basis of these data, the higher toxicity of peptide **5** in the panel screening should not pose as a major problem after intratumoral administration. Should the peptide enter into systemic circulation, our data suggest that peptide **5** will be broken down to noncytotoxic metabolites.

The instability of peptide **5** in human plasma represents a challenge for the determination of plasma protein binding properties and the plasma/blood cell partitioning which are both derived from the unbound concentration of peptide **5** in the plasma supernatant. When the broad spectrum serine protease inhibitor 4-(2-aminoethyl)benzenesulfonyl fluoride (AEBSF)[52] was added to the plasma at the start of the experiment, the recovery of peptide **5** was significantly increased from both spiked plasma and the supernatant, as the concentration of peptide **5** in the supernatant only fell from 176 ng/mL to 131 ng/mL after incubation for 20 h at 37 °C. The reduced degradation of peptide **5** by the addition of AEBSF allowed for an estimation of binding parameters; however the measured concentration in the supernatant does not represent all nonbound peptide **5** given that a certain portion of the peptide also degrades over the time span of the experiment. As a result the calculated degree of protein binding represents an upper limit for peptide **5** under these conditions. The extent of plasma protein binding was found to be independent of concentration for all three species, with similar results within the concentration range tested. A somewhat higher plasma protein binding was found for dog (<92 ± 2.3% bound) compared to human (<80 ± 4.2% bound) and rat (<75 ± 2.5% bound).

The mean blood/plasma ratio was determined after 60 min; hence the instability of peptide **5** is less significant in the determination of the binding to blood cells. The results are summarized in Table 4, which reveal that peptide **5** is moderately associated with red blood cells in human and rat whereas in dog the association to red blood cells is higher.

Table 4. Blood/Plasma Ratios at 60 min for Peptide 5

	rat	dog	human
blood/plasma ratio[a]	1.03	2.19	0.76
% peptide **5** associated with blood cells[a]	44	76	27

[a]Values as the mean of two independent measurements.

Preclinical Studies: CYP450 Inhibition and Stability in Hepatocytes. Peptide **5** was also assessed for its ability to inhibit human hepatic CYP450 enzymes by incubation with human liver microsomes and selective substrates for 9 CYP450 isoforms (see Table S4 for details). Incubation at different concentrations and with 5 or 30 min preincubation time revealed that peptide **5** is a relatively mild inhibitor of all 9 CYP450 isoforms included in this study (Table 6). The lower inhibitory effect against CYP1A2, 2A6, 2C19, 2D6, and 3A4 at 30 min incubation may indicate that peptide **5** is unstable over the longer preincubation time and/or is metabolized to a metabolite(s) that is less inhibitory than the parent peptide. Indeed, when peptide **5** was incubated with cryopreserved hepatocytes from rat and human, the concentration fell over time, and the half-life in both species was found to be around 1 h (Table 7). The difference in inhibitory effect after 5 and 30 min incubation, where none of the CYP450 isoforms were substantially more inhibited with time, suggests that peptide **5** is a mild and reversible inhibitor and that no irreversible CYP450 inhibitors are formed by metabolism of peptide **5**.

Mechanism of Action. Peptide **5** induces rapid killing of cancer cells in vitro,[7,53] while it has been found to be nontoxic toward human red blood cells (EC_{50} > 695 μM).[7] The low toxicity toward red blood cells may stem from the hydrophobic nature of their membranes compared to other types of eukaryotic cells.[54] The oncolytic activity of peptide **5** stems from a direct lytic effect on the plasma membrane in addition to permeabilization of the mitochondrial membrane, leading to cellular death by necrosis and release of tumor antigens.[8,53,55] Moreover, treatment of cancer cells with peptide **5** causes the release of several danger signals (DAMPs) that are associated with immunogenic cell death and stimulation of adaptive immune responses. Thus, peptide **5** induces an inflammatory

DOI: 10.1021/acs.jmedchem.5b02025
J. Med. Chem. XXXX, XXX, XXX−XXX

Table 5. Sequences and Biological Activity of Metabolites

compd	sequence	IC_{50} ± SD (μM)[a] MRC-5	A20
M1	Lys-Trp-Trp-Lys-Lys-Trp-Dip-Lys-NH_2	43.9 ± 19.3	13.5 ± 0.9
M2	Trp-Trp-Lys-Lys-Trp-Dip-Lys-NH_2	53.2 ± 21.2	20.3 ± 2.9
M3	Trp-Lys-Lys-Trp-Dip-Lys-NH_2	460 ± 71	247 ± 13

[a]Inhibitory concentration killing 50% of the cells (IC_{50}). Data from three or more independent measurements are presented as the mean ± SD.

Table 6. Inhibitory Activity of Peptide 5 against CYP450 Isoforms

enzyme	assay	IC_{50} (5 min)[a]	IC_{50} (30 min)[a]
CYP1A2	O-deethylation of phenacetin	37.9 ± 5.9	>100
CYP2A6	hydroxylation of coumarin	7.0 ± 2.2	26.3 ± 12.4
CYP2B6	hydroxylation of bupropion	27.7 ± 5.6	18.6 ± 2.0
CYP2C8	hydroxylation of paclitaxel	10.2 ± 1.1	7.9 ± 1.1
CYP2C9	hydroxylation of diclofenac	8.8 ± 2.0	8.7 ± 1.7
CYP2C19	hydroxylation of (*S*)-mephenytoin	23.3 ± 2.7	>100
CYP2D6	hydroxylation of bufuralol	21.9 ± 5.2	
CYP2E1	hydroxylation of chlorzoxazone	30.9 ± 5.2	30.0 ± 7.1
CYP3A4	hydroxylation of testosterone	9.3 ± 1.0	12.1 ± 1.1
CYP3A4	hydroxylation of midazolam	18.8 ± 5.6	63.7 ± 30.3

[a]Concentrations (in μM) resulting in 50% enzyme inhibition (IC_{50}). Values (±SD) from duplicate experiments reported.

Table 7. Stability of Peptide 5 in Cryopreserved Hepatocytes

compd	$t_{1/2}$[a] (min) rat	human	clearance[b] ((μL/min)/10^6 cells) rat	human
peptide **5**	71	64	20	22
testosterone[c]	2	4	811	333
midazolam[c]	27	>200	51	<7
4-methylumbelliferone[c]	4	11	373	127

[a]Half-lives obtained from two independent measurements presented as the mean. [b]Average intrinsic clearance. Data from two independent measurements presented as the mean. [c]The results for the reference compounds were as expected from historical data for these assays performed at BioFocus DPI, thus confirming the capacity of the hepatocytes for both phase I and phase II metabolism.

response and the subsequent activation and infiltration of immune cells such as cytotoxic $CB8^+$ T cells into the tumor parenchyma resulting in complete tumor regression and systemic tumor specific immune responses in preclinical tumor models.[7,8,53] On the basis of its unique oncolytic mode of action, peptide **5** has been introduced as a potential first in class oncolytic peptide.

CONCLUSION

The first in class oncolytic virus[3] has recently been approved, and this may pave the way for other types of local oncolytic immunotherapies. The potential first in class oncolytic peptide drug candidate, peptide **5**, was discovered through systematic design of 9-mer cationic peptides and screening of these for anticancer activity. We have found that the overall highest anticancer activity could be obtained by replacing Trp8 in a $(KKWW)_2K$-NH_2 sequence with the more bulky unnatural Dip amino acid.

Furthermore, peptide **5** was found to be equipotent against drug-resistant cancer cells, nontoxic toward red blood cells, showed high plasma protein binding, and was quite rapidly degraded to nontoxic metabolites. Hence, peptide **5** should be ideally suited for intratumoral administration.

Indeed, intratumoral administration of peptide **5** has resulted in complete regression and systemic tumor specific immune responses in several preclinical models. Therefore, peptide **5** is currently being tested in a clinical phase I/IIa study,[10] showing tumor regression and enhanced infiltration of immune cells in injected lesions.[56]

EXPERIMENTAL SECTION

Peptide Synthesis. All peptides were prepared at room temperature in an automated fashion using standard Fmoc-based solid-phase peptide synthesis on a Rink amide AM resin (NovaBiochem). Briefly, each amino acid was coupled using HBTU or PyBOP as coupling reagent and DIPEA as base in DMF for 30−60 min. Removal of the Fmoc-protecting group after each coupling step was facilitated using 20% piperidine in DMF. Peptides were cleaved off from the resin and deprotected using a mixture of trifluoroacetic acid, water, and triisopropylsilane (95:2.5:2.5, v/v/v) for 2.5−3 h. The resin was filtered off using a glass-sintered filter, washed with a fresh portion of trifluoroacetic acid, and the filtrate was evaporated under reduced pressure. Crude peptides were precipitated by addition of cold diethyl ether. The ether layer was removed and the solid residue triturated two times with diethyl ether and dried under reduced pressure. The crude peptides were purified by reversed phase HPLC (RP-HPLC) and lyophilized. Purified peptides were analyzed by analytical RP-HPLC, and the integrity of the peptides was checked by positive ion electrospray ionization mass spectrometry (ESI-MS). Analytical data are given in Table S1. All peptides tested were found to be of >95% purity (RP-HPLC 214/254 nm). Peptide **5** (acetate salt) for preclinical studies was provided by Bachem (Bubendorf, Switzerland).

Cell Lines Initial SAR Study. A20 (ATCC, TIB-208), a naturally occurring murine B cell lymphoma of Balb/c origin, and AT84 (kindly provided by Prof. Shillitoe, Upstate Medical University, Syracuse, NY, USA), a naturally occurring murine squamous cell carcinoma of C3H origin, were both cultured in RPMI-1640 containing 2 mM L-glutamine and 1.5 g/L sodium bicarbonate. The A20 culture medium was further modified to contain 4.5 g/L glucose, 10 mM HEPES, 1.0 mM sodium pyruvate, and 0.05 mM 2-mercaptoethanol. MRC-5 (ATCC, CCL-171), a human embryonic lung fibroblast cell line, was cultured in MEM containing 2 mM L-glutamine. All culture media were supplemented with 10% fetal bovine serum and were without antibiotics. Cell cultures were maintained in a humidified atmosphere of 5% CO_2 and >95% humidity at 37 °C and tested for both mycoplasma and other pathogens (RapidMAP-27, Taconic, Denmark) or mycoplasma alone.

Cell Lines Panel Screening. These experiments were performed by Oncodesign S.A. (Dijon, France). Tumor cells were grown as adherent monolayers or as suspensions at 37 °C in a humidified atmosphere (5% CO_2, 95% air). The culture medium was RPMI-1640 containing 2 mM L-glutamine and supplemented with 10% fetal bovine serum (FBS). Cells were counted in a hemocytometer and their viability was assessed by 0.25% trypan blue exclusion. Mycoplasma detection was performed using the MycoAlert mycoplasma detection

DOI: 10.1021/acs.jmedchem.5b02025
J. Med. Chem. XXXX, XXX, XXX−XXX

kit (Lonza, Verviers, Belgium) in accordance with the manufacturer instructions.

In Vitro Cytotoxicity. A colorimetric 3-(4,5-dimethylthiazol-2-yl)-2,5-diphenyltetrazodium bromide (MTT) viability assay[57] was employed to assess the in vitro cytotoxicity toward MRC-5, AT20, and AT84 cells following the same protocol as previously reported.[7] For all other cell lines (at Oncodesign S.A., Dijon, France), a colorimetric 3-(4,5-dimethylthiazol-2-yl)-5-(3-carboxymethoxyphenyl)-2-(4-sulfophenyl)-2*H*-tetrazolium (MTS) assay[58] with phenazine methosulfate (PMS) as electron coupling reagent was used. The adherent cell lines were washed once with 200 μL of FBS-free culture medium before treatment. Tumor cells were plated in 96-well flat-bottom microtitration plates (Nunc, Dutscher, Brumath, France) and incubated at 37 °C for 24 h before treatment in 190 μL of drug-free and FBS-free culture medium. Tumor cells were incubated for 4 h with 10 concentrations of compounds in 1/4 dilution step with a top dose of 400 μM (range 4×10^{-4} to 4×10^{-10} M), with 1% (final concentration) Triton X-100 as positive control and FBS-free culture medium as negative control. The cells (190 μL) were incubated in a 200 μL final volume of FBS-free culture medium containing test substances at 37 °C under 5% CO_2. Three independent experiments were performed, each concentration being issued from quadruplicate. Control cells were treated with vehicle alone. At the end of the cell treatment, an amount of 40 μL of a 0.22 μm filtered freshly combined solution of MTS (20 mL at 2 mg/mL) and PMS (1 mL at 0.92 mg/mL) in Dulbecco's phosphate buffered saline (DPBS) was added to each well. Culture plates were incubated for 2 h at 37 °C. Absorbency (OD) was measured at 490 nm in each well using VICTOR^3 1420 multilabeled counter (Wallac, PerkinElmer, Courtaboeuf, France). The dose response inhibition of proliferation (IC) was expressed as IC = $(OD_{drug}/OD_{blank}) \times 100$, where the OD values which are the mean of four experimental measurements were plotted using XLFit 3 (IDBS, United Kingdom) and IC_{50} values were determined using the XLFit 3 software from semilog curves derived from three independent measurements.

Plasma Protein Binding. These experiments were performed by Quotient Bioresearch Ltd. (Rushden, U.K.). Fresh control human whole blood was collected into lithium heparin tubes from healthy male and female volunteers who had taken no medication during the previous 7 days and no alcohol for 24 h. The blood samples were centrifuged (3000*g*, 10 min), and the plasma was harvested. Plasma was pooled and was stored frozen (approximately −80 °C) until required. Plasma (whole blood had been collected into lithium heparin tubes) from rat (Han Wistar) and dog (Beagle) was purchased from Matrix Biologicals Ltd. (Cambridge, U.K.). Plasma was pooled from at least 3 male and 3 female animals per species and was stored frozen (approximately −80 °C) until required. Peptide **5** (25 μL of a solution containing either 20, 50, or 100 μg/mL peptide dissolved in water) was added to plasma solutions from rat, dog, and human (2.475 mL) containing AEBSF (1 mg/mL) giving 200, 500, or 1000 ng/mL as final concentration of peptide **5** (in duplicate). Plasma samples containing peptide **5** (approximately 1.8 mL) were loaded into ultracentrifuge tubes and were separated in a Sorvall Discovery 90SE ultracentrifuge (45 000 rpm at 37 °C for 20 h with acceleration and deceleration set to 9 and 4, respectively). Following centrifugation, each supernatant (approximately 0.5 mL) was carefully removed by a syringe with an attached hypodermic needle whose tip was placed just below the surface. The supernatant was transferred into an Eppendorf tube, and the samples were stored frozen prior to analysis. The amount of peptide **5** in each sample was quantified using LC−MS/MS (see method 1 below), and the extent of plasma protein binding was calculated according to the formula % bound = $[(C - C_S)/C] \times 100$, where C is the concentration in plasma and C_S is the measured concentration in the supernatant.

Plasma/Blood Partitioning. These experiments were performed by Quotient Bioresearch Ltd. (Rushden, U.K.). Fresh whole blood was collected from human (for details see above), dog (Quotient Bioresearch Ltd., Rushden, U.K., beagle stock animals), and rat (supplied by Charles River UK Ltd., Margate, Kent, U.K.). Blood was collected from at least 3 male and 3 female donors/animals. Aliquots of whole blood from the different species were pooled, and the pooled blood was stored at room temperature for a maximum of 2 h until use. Peptide **5** (20 μL of a solution containing 20 μg/mL) was added to aliquots of whole blood (10 × 0.98 mL) to give a peptide concentration of 200 ng/mL. The blood was incubated at approximately 37 °C for 0, 10, 30, 60, and 120 on a rotary mixer. After incubation, a packed cell volume determination was made (determination of hematocrit) and aliquots of blood were analyzed by LC−MS/MS (see method 1 below) to determine the concentration of peptide **5**. The remainder of the blood samples was centrifuged to prepare plasma, and aliquots of plasma were analyzed by LC−MS/MS to determine the concentration of peptide **5**. The plasma/blood cell partitioning was determined using the formula blood/plasma ratio = C_b/C, where C_b and C are the blood and plasma concentrations of peptide **5**, respectively. The partition coefficient was determined using the formula partition coefficient = $\{[C(1 - H)]/C_b\} \times 100$, where H is the hematocrit (packed cell volume) as a decimal.

Half-Life in Human Plasma. Blood samples were collected from healthy volunteers in heparin treated vacutainers, and plasma was collected after centrifugation at 1500 rpm for 10 min. Peptide **5** (250 μL of a 1 mg/mL solution in isotonic saline) and plasma (1000 μL) were carefully mixed, and aliquots of 125 μL were sampled at different time intervals. To each sample were added water (0.5 mL containing 1% TFA) and an internal standard (25 μL of a l mg/mL solution of tripeptide derivative Arg-Bip-Arg-NHiPr in water), and the mixture was applied onto a preconditioned (methanol) and equilibrated (water with 1% TFA) 1 cc OASIS HLB solid phase extraction column (Waters). The column was washed with water (2 mL, containing 1% TFA) and eluted with a mixture of water and acetonitrile containing 1% TFA (30:70, 2 × 1 mL). Each sample (in all cases only the first fraction contained the analyte) was analyzed by RP-HPLC with UV detection at 214 nm. Samples showing significant presence of metabolites were further analyzed by LC−MS. The half-life of peptide **5** was calculated using the Cornell University medical calculator.[59]

CYP450 Inhibition. These experiments were performed by Quotient Bioresearch Ltd. (Rushden, U.K.). Pooled human liver microsomes (from 50 individual donors of mixed gender) supplied by Xenotech (Xenotech, LLC, Lenexa, KS, USA) at a microsomal protein concentration of 20 mg/mL were stored at approximately −80 °C. Stock solutions of peptide **5** (2, 20, 200, and 2000 μM in water) were added to microsomes (in 100 mM phosphate buffer, pH 7.4) containing β-NADPH (2 mM final concentration) at 0.1 mg/mL (CYP2A6, CYP2C8, CYP2C9, CYP2E1, and CYP3A4) or 0.3 mg/mL (CYP1A2, CYP2B6, CYP2C19, and CYP2D6) microsomal protein concentration at final incubation concentrations of 0, 0.01, 0.1, 1, 10, and 100 μM and incubated at approximately 37 °C for 5 or 30 min prior to the addition of selective substrates (see Table S4). The final assay volume was 400 μL, and all experiments were performed in duplicate. Positive control experiments where a known inhibitor selective for each of the CYP450 isoforms (see Table S4 for details) were performed using the same setup. Microsomal reactions were terminated by addition of an aliquot of the assay solution into an equal volume of methanol containing an internal standard (see Table S4 for details) on a 96-well Mulitiscreen Solvinert filter plate (hydrophilic, 0.45 μm). An equal amount of fresh methanol was added prior to filtration into a receiver plate under vacuum. Samples were stored at approximately 4 °C and analyzed using LC−MS/MS (see method 1 below) on the same day. Quantification of metabolites was performed by interpolation from a standard curve, which was prepared using the relevant metabolite standard. The rate of metabolite formation in each experiment containing peptide **5** was compared to the rate of metabolite formation in the absence of peptide **5**, and in cases where more than 50% inhibition was observed at ≤100 μM, an IC_{50} value was calculated using Grafit, version 5.0.6, from semilog curves derived from the two independent measurements.

Stability in Hepatocytes. These experiments were performed by BioFocus DPI (Romainville, France). Peptide **5** was incubated (1 μM initial concentration) with pooled and cryopreserved rat and human hepatocytes supplied by Celsis (Leipzig, Germany) at a cell density of 0.5 million cells/mL at approximately 37 °C. 100 μL samples were

DOI: 10.1021/acs.jmedchem.5b02025
J. Med. Chem. XXXX, XXX, XXX−XXX

taken after 0, 10, 20, 45, and 90 min and the reactions terminated by addition of 100 μL of 20% TFA containing modified substance P ([D-Trp^{7,9,10}] substance P) as internal standard. Samples were centrifuged and the supernatant fractions analyzed by LC−MS/MS (see method 2 below). The experiments were carried out in duplicate. Testosterone, midazolam, and 4-methylumbelliferone were used as positive controls for the metabolic capacity (phase I oxidation and phase II conjugation reactions) of the cryopreserved preparations. The instrument responses (peak height) were referenced to the zero time-point samples (as 100%) in order to determine the percentage of remaining peptide **5**. The half-life was calculated using the formula $t_{1/2}$ (min) = $-0.693/\lambda$, where λ is the slope of the ln concentration vs time curve. In vitro clearance (Cl_{int}) as (μL/min)/million cells was calculated using the formula $Cl_{int} = 0.693 \times 1/t_{1/2}$ (min) $\times V_{inc}$ (μL)/million cells, where $t_{1/2}$ is the half-life and V_{inc} is the incubation volume.

LC−MS/MS Quantification. *Method 1.* The analysis was carried out on a SCIEX API 5000 mass spectrometer using an Onyx Monolithic C18 (50 mm × 2.0 mm) analytical column with a fast gradient elution using a mobile phase of acetonitrile/isopropanol (50/50 v/v) and 10 mM ammonium formate (pH 3). The flow rate was 0.55 mL, and the run time was 3.5 min. The analyte and the internal standard ($^{13}C_6$,$^{15}N_2$-peptide **5**) were ionized using the TurbolonSpray interface in positive ion mode. The concentration of the analyte was determined by chromatographic integration of selected fragmentation transitions (MRM).

Method 2. The analysis was carried out on a Waters Quattro Micro mass spectrometer using an XBridge C18 (50 mm × 2.1 mm) analytical column with a fast gradient elution using a mobile phase of 0.2% formic acid in acetonitrile and 10 mM ammonium formate (pH 3). The flow rate was 0.5 mL, and the run time was 5 min. The analyte and the internal standard (D-Trp^{7,9,10}-substance P) was ionized using the API interface in positive ion mode. The concentration of the analyte was determined by chromatographic integration of selected fragmentation transitions (MRM).

■ ASSOCIATED CONTENT

Supporting Information

The Supporting Information is available free of charge on the ACS Publications website at DOI: 10.1021/acs.jmedchem.5b02025.

Summary of analytical data for peptides, details regarding cancer cell lines, results from panel screening, details on CYP450 substrates and inhibitors (PDF)

■ AUTHOR INFORMATION

Corresponding Authors

*B.E.H.: phone, (+47) 55583468; e-mail, bengt-erik.haug@uib.no.

*Ø.R.: phone, (+47) 77675500; e-mail, Oystein.Rekdal@lytixbiopharma.com.

Present Addresses

⊥B.E.H.: University of Bergen, NO-5007 Bergen, Norway.

#L.T.E.: The Tumor Biology Research Group, Faculty of Health Sciences, UIT, The Arctic University of Norway, Breivika, NO-9037 Tromsø, Norway.

∇K.B.: NorStruct, Department of Chemistry, Faculty of Science and Technology, Science Park 3, Sykehusveien 23, UIT, The Arctic University of Norway, Breivika, NO-9037 Tromsø, Norway.

Author Contributions

The manuscript was written through contributions of all authors. All authors have given approval to the final version of the manuscript.

Notes

The authors declare the following competing financial interest(s): B.E.H. is a shareholder in Lytix Biopharma AS. B.M. is a shareholder in and employed by Lytix Biopharma AS. K.A.C. receives financial support from and is a shareholder in Lytix Biopharma AS. J.S.S. and Ø.R. are co-founders, shareholders, and employees of Lytix Biopharma AS. W.S. receives financial support from Lytix Biopharma AS.

■ ACKNOWLEDGMENTS

The authors thank Mari Wikman, Inger Lindin, and Johann Eksteen for technical assistance related to peptide syntheses and in vitro assays. This work was funded in part by The Research Council of Norway.

■ ABBREVIATIONS USED

AEBSF, 4-(2-aminoethyl)benzenesulfonyl fluoride; Ath, 9-anthracenylalanine; Bip, biphenylalanine; Dab, (*S*)-2,4-diaminobutyric acid; DAMP, danger-associated molecular pattern molecule; Dap, (*S*)-2,3-diaminopropionic acid; Dip, 3,3-diphenylalanine; FBS, fetal bovine serum; LFcinB, bovine lactoferricin; MTS, 3-(4,5-dimethylthiazol-2-yl)-5-(3-carboxymethoxyphenyl)-2-(4-sulfophenyl)-2*H*-tetrazolium; PMS, phenazine methosulfate; MTT, 3-(4,5-dimethylthiazol-2-yl)-2,5-diphenyltetrazodium bromide; 1-Nal, 1-naphthylalanine; 2-Nal, 2-naphthylalanine

■ REFERENCES

(1) Eggermont, A. M. M.; Kroemer, G.; Zitvogel, L. Immunotherapy and the concept of a clinical cure. *Eur. J. Cancer* **2013**, *49*, 2965−2967.

(2) Chiocca, E. A.; Rabkin, S. D. Oncolytic viruses and their application to cancer immunotherapy. *Cancer Immunol. Res.* **2014**, *2*, 295−300.

(3) Andtbacka, R. H. I.; Kaufman, H. L.; Collichio, F.; Amatruda, T.; Senzer, N.; Chesney, J.; Delman, K. A.; Spitler, L. E.; Puzanov, I.; Agarwala, S. S.; Milhem, M.; Cranmer, L.; Curti, B.; Lewis, K.; Ross, M.; Guthrie, T.; Linette, G. P.; Daniels, G. A.; Harrington, K.; Middleton, M. R.; Miller, W. H.; Zager, J. S.; Ye, Y.; Yao, B.; Li, A.; Doleman, S.; VanderWalde, A.; Gansert, J.; Coffin, R. Talimogene laherparepvec improves durable response rate in patients with advanced melanoma. *J. Clin. Oncol.* **2015**, *33*, 2780−2788.

(4) Al-Benna, S.; Shai, Y.; Jacobsen, F.; Steinstraesser, L. Oncolytic activities of host defense peptides. *Int. J. Mol. Sci.* **2011**, *12*, 8027−8051.

(5) Kroemer, G.; Galluzzi, L.; Kepp, O.; Zitvogel, L. Immunogenic cell death in cancer therapy. *Annu. Rev. Immunol.* **2013**, *31*, 51−72.

(6) Berge, G.; Eliassen, L. T.; Camilio, K. A.; Bartnes, K.; Sveinbjørnsson, B.; Rekdal, Ø. Therapeutic vaccination against a murine lymphoma by intratumoral injection of a cationic anticancer peptide. *Cancer Immunol. Immunother.* **2010**, *59*, 1285−1294.

(7) Camilio, K. A.; Berge, G.; Ravuri, C. S.; Rekdal, Ø.; Sveinbjørnsson, B. Complete regression and systemic protective immune responses obtained in B16 melanomas after treatment with LTX-315. *Cancer Immunol. Immunother.* **2014**, *63*, 601−613.

(8) Camilio, K. A.; Rekdal, Ø.; Sveinbjörnsson, B. LTX-315 (Oncopore) A short synthetic anticancer peptide and novel immunotherapeutic agent. *OncoImmunology* **2014**, *3*, e29181−e29183.

(9) ClinicalTrials.gov NCT01058616.

(10) ClinicalTrials.gov NCT01986426.

(11) Tomita, M.; Bellamy, W.; Takase, M.; Yamauchi, K.; Wakabayashi, H.; Kawase, K. Potent antibacterial peptides generated by pepsin digestion of bovine lactoferrin. *J. Dairy Sci.* **1991**, *74*, 4137−4142.

(12) Bellamy, W.; Takase, M.; Yamauchi, K.; Wakabayashi, H.; Kawase, K.; Tomita, M. Identification of the bactericidal domain of

DOI: 10.1021/acs.jmedchem.5b02025
J. Med. Chem. XXXX, XXX, XXX−XXX

lactoferrin. *Biochim. Biophys. Acta, Protein Struct. Mol. Enzymol.* **1992**, *1121*, 130−136.
(13) Rekdal, Ø.; Andersen, J.; Vorland, L. H.; Svendsen, J. S. Construction and synthesis of lactoferricin derivatives with enhanced antibacterial activity. *J. Pept. Sci.* **1999**, *5*, 32−45.
(14) Zasloff, M. Antimicrobial peptides of multicellular organisms. *Nature* **2002**, *415*, 389−395.
(15) Ganz, T. The role of antimicrobial peptides in innate immunity. *Integr. Comp. Biol.* **2003**, *43*, 300−304.
(16) Yoo, Y.-C.; Watanabe, R.; Koike, Y.; Mitobe, M.; Shimazaki, K.-i.; Watanabe, S.; Azuma, I. Apoptosis in human leukemic cells induced by lactoferricin, a bovine milk protein-derived peptide: Involvement of reactive oxygen species. *Biochem. Biophys. Res. Commun.* **1997**, *237*, 624−628.
(17) Eliassen, L. T.; Berge, G.; Sveinbjornsson, B.; Svendsen, J. S.; Vorland, L. H.; Rekdal, O. Evidence for a direct antitumor mechanism of action of bovine lactoferricin. *Anticancer Res.* **2002**, *22*, 2703−2710.
(18) Mader, J. S.; Salsman, J.; Conrad, D. M.; Hoskin, D. W. Bovine lactoferricin selectively induces apoptosis in human leukemia and carcinoma cell lines. *Mol. Cancer Ther.* **2005**, *4*, 612−624.
(19) Richardson, A.; de Antueno, R.; Duncan, R.; Hoskin, D. W. Intracellular delivery of bovine lactoferricin's antimicrobial core (RRWQWR) kills T-leukemia cells. *Biochem. Biophys. Res. Commun.* **2009**, *388*, 736−741.
(20) Hilchie, A. L.; Vale, R.; Zemlak, T. S.; Hoskin, D. W. Generation of a hematologic malignancy-selective membranolytic peptide from the antimicrobial core (RRWQWR) of bovine lactoferricin. *Exp. Mol. Pathol.* **2013**, *95*, 192−198.
(21) Hoskin, D. W.; Ramamoorthy, A. Studies on anticancer activities of antimicrobial peptides. *Biochim. Biophys. Acta, Biomembr.* **2008**, *1778*, 357−375.
(22) Riedl, S.; Zweytick, D.; Lohner, K. Membrane-active host defense peptides − Challenges and perspectives for the development of novel anticancer drugs. *Chem. Phys. Lipids* **2011**, *164*, 766−781.
(23) Gaspar, D.; Veiga, A. S.; Castanho, M. A. R. B. From antimicrobial to anticancer peptides. A review. *Front. Microbiol.* **2013**, *4*, 1−16.
(24) Rapaport, D.; Shai, Y. Interaction of fluorescently labeled pardaxin and its analogues with lipid bilayers. *J. Biol. Chem.* **1991**, *266*, 23769−23775.
(25) Ludtke, S. J.; He, K.; Heller, W. T.; Harroun, T. A.; Yang, L.; Huang, H. W. Membrane pores induced by magainin. *Biochemistry* **1996**, *35*, 13723−13728.
(26) Gazit, E.; Miller, I. R.; Biggin, P. C.; Sansom, M. S. P.; Shai, Y. Structure and orientation of the mammalian antibacterial peptide cecropin P1 within phospholipid membranes. *J. Mol. Biol.* **1996**, *258*, 860−870.
(27) Miteva, M.; Andersson, M.; Karshikoff, A.; Otting, G. Molecular electroporation: a unifying concept for the description of membrane pore formation by antibacterial peptides, exemplified with NK-lysin. *FEBS Lett.* **1999**, *462*, 155−158.
(28) Pokorny, A.; Birkbeck, T. H.; Almeida, P. F. F. Mechanism and kinetics of δ-lysin interaction with phospholipid vesicles. *Biochemistry* **2002**, *41*, 11044−11056.
(29) Wimley, W. C. Describing the mechanism of antimicrobial peptide action with the interfacial activity model. *ACS Chem. Biol.* **2010**, *5*, 905−917.
(30) Wimley, W. C.; Hristova, K. Antimicrobial peptides: successes, challenges and unanswered questions. *J. Membr. Biol.* **2011**, *239*, 27−34.
(31) Gee, M. L.; Burton, M.; Grevis-James, A.; Hossain, M. A.; McArthur, S.; Palombo, E. A.; Wade, J. D.; Clayton, A. H. A. Imaging the action of antimicrobial peptides on living bacterial cells. *Sci. Rep.* **2013**, *3*, 1557.
(32) Brogden, K. A. Antimicrobial peptides: pore formers or metabolic inhibitors in bacteria? *Nat. Rev. Microbiol.* **2005**, *3*, 238−250.
(33) Utsugi, T.; Schroit, A. J.; Connor, J.; Bucana, C. D.; Fidler, I. J. Elevated expression of phosphatidylserine in the outer-membrane leaflet of human tumor-cells and recognition by activated human blood monocytes. *Cancer Res.* **1991**, *51*, 3062−3066.
(34) Schibli, D. J.; Nguyen, L. T.; Kernaghan, S. D.; Rekdal, Ø.; Vogel, H. J. Structure-function analysis of tritrpticin analogs: potential relationships between antimicrobial activities, model membrane interactions, and their micelle-bound NMR structures. *Biophys. J.* **2006**, *91*, 4413−4426.
(35) Rekdal, Ø.; Haug, B. E.; Kalaaji, M.; Hunter, H. N.; Lindin, I.; Israelsson, I.; Solstad, T.; Yang, N.; Brandl, M.; Mantzilas, D.; Vogel, H. J. Relative spatial positions of tryptophan and cationic residues in helical membrane-active peptides determine their cytotoxicity. *J. Biol. Chem.* **2012**, *287*, 233−244.
(36) Riedl, S.; Rinner, B.; Schaider, H.; Lohner, K.; Zweytick, D. Killing of melanoma cells and their metastases by human lactoferricin derivatives requires interaction with the cancer marker phosphatidylserine. *BioMetals* **2014**, *27*, 981−997.
(37) Riedl, S.; Leber, R.; Rinner, B.; Schaider, H.; Lohner, K.; Zweytick, D. Human lactoferricin derived di-peptides deploying loop structures induce apoptosis specifically in cancer cells through targeting membranous phosphatidylserine. *Biochim. Biophys. Acta, Biomembr.* **2015**, *1848*, 2918−2931.
(38) Lau, Q. Y.; Ng, F. M.; Cheong, J. W. D.; Yap, Y. Y. A.; Tan, Y. Y. F.; Jureen, R.; Hill, J.; Chia, C. S. B. Discovery of an ultra-short linear antibacterial tetrapeptide with anti-MRSA activity from a structure−activity relationship study. *Eur. J. Med. Chem.* **2015**, *105*, 138−144.
(39) Ausbacher, D.; Svineng, G.; Hansen, T.; Strøm, M. B. Anticancer mechanisms of action of two small amphipathic $\beta^{2,2}$-amino acid derivatives derived from antimicrobial peptides. *Biochim. Biophys. Acta, Biomembr.* **2012**, *1818*, 2917−2925.
(40) Hansen, T.; Alst, T.; Havelkova, M.; Strøm, M. B. Antimicrobial activity of small β-peptidomimetics based on the pharmacophore model of short cationic antimicrobial peptides. *J. Med. Chem.* **2010**, *53*, 595−606.
(41) Tørfoss, V.; Ausbacher, D.; Cavalcanti-Jacobsen, C. d. A.; Hansen, T.; Brandsdal, B.-O.; Havelkova, M.; Strøm, M. B. Synthesis of anticancer heptapeptides containing a unique lipophilic $\beta^{2,2}$-amino acid building block. *J. Pept. Sci.* **2012**, *18*, 170−176.
(42) Tørfoss, V.; Isaksson, J.; Ausbacher, D.; Brandsdal, B.-O.; Flaten, G. E.; Anderssen, T.; Cavalcanti-Jacobsen, C. d. A.; Havelkova, M.; Nguyen, L. T.; Vogel, H. J.; Strøm, M. B. Improved anticancer potency by head-to-tail cyclization of short cationic anticancer peptides containing a lipophilic $\beta^{2,2}$-amino acid. *J. Pept. Sci.* **2012**, *18*, 609−619.
(43) Eliassen, L. T.; Haug, B. E.; Berge, G.; Rekdal, Ø. Enhanced antitumour activity of 15-residue bovine lactoferricin derivatives containing bulky aromatic amino acids and lipophilic N-terminal modifications. *J. Pept. Sci.* **2003**, *9*, 510−517.
(44) Haug, B. E.; Strøm, M. B.; Svendsen, J. S. M. The medicinal chemistry of short lactoferricin-based antibacterial peptides. *Curr. Med. Chem.* **2007**, *14*, 1−18.
(45) Yang, N.; Rekdal, Ø.; Stensen, W.; Svendsen, J. S. Enhanced antitumor activity and selectivity of lactoferrin-derived peptides. *J. Pept. Res.* **2002**, *60*, 187−197.
(46) Haug, B. E.; Skar, M. L.; Svendsen, J. S. Bulky aromatic amino acids increase the antibacterial activity of 15-residue bovine lactoferricin derivatives. *J. Pept. Sci.* **2001**, *7*, 425−432.
(47) Isidro-Llobet, A.; Álvarez, M.; Albericio, F. Amino acid-protecting groups. *Chem. Rev.* **2009**, *109*, 2455−2504.
(48) Lan, Y.; Langlet-Bertin, B.; Abbate, V.; Vermeer, L. S.; Kong, X.; Sullivan, K. E.; Leborgne, C.; Scherman, D.; Hider, R. C.; Drake, A. F.; Bansal, S. S.; Kichler, A.; Mason, A. J. Incorporation of 2,3-diaminopropionic acid into linear cationic amphipathic peptides produces pH-sensitive vectors. *ChemBioChem* **2010**, *11*, 1266−1272.
(49) Yang, S.-T.; Shin, S. Y.; Lee, C. W.; Kim, Y.-C.; Hahm, K.-S.; Kim, J. I. Selective cytotoxicity following Arg-to-Lys substitution in tritrpticin adopting a unique amphipathic turn structure. *FEBS Lett.* **2003**, *540*, 229−233.
(50) Vogel, H. J.; Schibli, D. J.; Jing, W.; Lohmeier-Vogel, E. M.; Epand, R. F.; Epand, R. M. Towards a structure-function analysis of

DOI: 10.1021/acs.jmedchem.5b02025
J. Med. Chem. XXXX, XXX, XXX−XXX

bovine lactoferricin and related tryptophan- and arginine-containing peptides. *Biochem. Cell Biol.* **2002**, *80*, 49−63.

(51) Nguyen, L. T.; de Boer, L.; Zaat, S. A. J.; Vogel, H. J. Investigating the cationic side chains of the antimicrobial peptide tritrpticin: Hydrogen bonding properties govern its membrane-disruptive activities. *Biochim. Biophys. Acta, Biomembr.* **2011**, *1808*, 2297−2303.

(52) Powers, J. C.; Asgian, J. L.; Ekici, Ö. D.; James, K. E. Irreversible inhibitors of serine, cysteine, and threonine proteases. *Chem. Rev.* **2002**, *102*, 4639−4750.

(53) Eike, L.-M.; Yang, N.; Rekdal, Ø.; Sveinbjørnsson, B. The oncolytic peptide LTX-315 induces cell death and DAMP release by mitochondria distortion in human melanoma cells. *Oncotarget* **2015**, *6*, 34910−34923.

(54) Gennis, R. B. *Biomembranes: Molecular Structure and Function*; Springer-Verlag: New York, 1989.

(55) Zhou, H.; Forveille, S.; Sauvat, A.; Sica, V.; Izzo, V.; Durand, S.; Müller, K.; Liu, P.; Zitvogel, L.; Rekdal, Ø.; Kepp, O.; Kroemer, G. The oncolytic peptide LTX-315 kills cancer cells through Bax/Bak-regulated mitochondrial membrane permeabilization. *Oncotarget* **2015**, *6*, 26599−26614.

(56) Spicer, J.; Awada, A.; Brunsvig, P. F.; Kristeleit, R.; Jøssang, D. E.; Saunders, A.; Olsen, W. M.; Nicolaisen, B.; Rekdal, Ø.; Laruelle, M.; Marjuadi, F.; Vakili, J.; Aftimos, P.; Barthelemy, P.; Deva, S.; Jebsen, N. L.; Baurain, J.-F. Intra-tumoural treatment with LTX-315, an oncolytic peptide immunotherapy, in patients with advanced metastatic disease induces infiltration of CD8 effectors T-cells and regression in some injected tumors. Presented at the 18th European Cancer Congress, September 25−29, 2015, Vienna, Austria.

(57) Mosmann, T. Rapid colorimetric assay for cellular growth and survival: application to proliferation and cytotoxicity assays. *J. Immunol. Methods* **1983**, *65*, 55−63.

(58) Cory, A. H.; Owen, T. C.; Barltrop, J. A.; Cory, J. G. Use of an aqueous soluble tetrazolium/formazan assay for cell growth assays in culture. *Cancer Commun.* **1991**, *3*, 207−212.

(59) Calculation of half-life using the Cornell University medical calculator: http://www-users.med.cornell.edu/~spon/picu/calc/halfcalc.htm (accessed March 3, 2016).

DOI: 10.1021/acs.jmedchem.5b02025
J. Med. Chem. XXXX, XXX, XXX−XXX